

Extracting more signal at high intensities in oligonucleotide arrays

Felix Naef¹, Nicholas D. Socci² and Marcelo Magnasco¹

¹Center for Studies in Physics and Biology, ²Laboratory for Molecular Genetics,
Rockefeller University, 1230 York Avenue, NY 10021

June 17, 2019

Abstract

Motivation: The majority of work in the analysis of microarray data has focused on improving the signal to noise ratio in the low concentration region. However, improvements are also possible at the opposite extreme: at high concentrations. This problem appears to have been neglected for two reasons: first, it is counter-intuitive to expect problems in what appears to be the cleanest region and second, the data necessary to identify and develop improvements has not been widely available. Fortunately, the situation has changed and precise calibration data produced by Affymetrix which enables the analysis of signals over a broad range of concentrations. Using this data, we address the question: “Where on the concentration/intensity scale are we able (or unable) to detect fold changes of 2 and greater?”

Results: First, we empirically demonstrate that while current techniques are capable of detecting changes in the low to middle concentration range, the situation is quite different for high concentrations. Specifically, in this regime, expression changes as large as 4 fold are severely compressed, and changes of 2 are often undetectable. However, a feature of GeneChips is that transcripts are probed by a set of sequence fragments having a wide range of affinities. The key to improving the accuracy in a given intensity range, is choosing those probes that are most responsive in that range. Utilizing this property and borrowing ideas from the theory of local linear embeddings (LLE) we present a new approach capable of reducing the compression at high intensity.

Availability: Program source code will be sent electronically upon request.

Contact: felix@funes.rockefeller.edu;
soccin@rockefeller.edu;
marcelo@zahir.rockefeller.edu

Introduction

High-density oligonucleotide arrays manufactured by Affymetrix are currently among the most sensitive and reliable microarray technology (Chee *et al.*, 1996; Lipshutz *et al.*, 1999) available. Based on a photolithographic oligonucleotide deposition process, labeled and amplified mRNA transcripts are probed by 28-40 short DNA sequence each 25 bases long. The probes are preferentially picked near the 3' end of the mRNA sequence, because of the limited efficiencies of reverse transcription enzymes. In addition, the probes come in two varieties: half are perfect matches (*PM*) identical to templates found in databases, and the other half are single mismatches (*MM*), carrying a single base substitution in the middle (13th) base of the sequence. *MM* probes were introduced to serve as controls for non-specific hybridization, and it was thought that the actual signal (the target's mRNA concentration) would be proportional to the difference of match versus mismatch (*PM-MM*). We shall confirm below that as a first approximation, this subtraction procedure is *the most reasonable* choice, leading to remarkably good results in the *low to mid concentration range*. However, we shall show that for high concentrations, the signal tends to be suppressed when using differentials.

This result is likely to sound surprising and counter-intuitive to many, which we believe is rooted in the following widespread interpretation of hybridization data. Namely, when examining a typical plot of the data from two replicated conditions (Figure 1a) most would immediately focus on the low intensity region, and observe how noisy this regime appears to be in comparison to the much cleaner high-intensity range. However, matters turn out to be more complex and we shall argue this view is at least partly incorrect and often misleading. Turning to a comparison of two different conditions (Figure 1b), we notice that the noise envelope is essentially unchanged, and that real changes appear as points lying

distinctively outside the noise cloud. Repeating this exercise on many different conditions, we would then conclude that the high intensity data is almost always very tightly scattered about the diagonal, and that there are rarely genes in that region that show fold changes greater than, say, 1.5 or 2. Should we then conclude that there is no interesting biology occurring at high intensities, or perhaps that all highly expressed genes are “house keeping” genes? The answer is probably no. In fact we shall show evidence that the high-intensity regime is strongly compressive, and that real changes are often hidden. This saturation effect can actually be observed in Affymetrix’s own data¹ although the issue is not discussed there.

The explanation for the compression effect invokes non-linear probe affinities and chemical saturation, which are *not* saturation effects resulting from the photodetector threshold. Issues related to photodetection saturation present a separate problem, and they have essentially been fixed by Affymetrix by lowering the laser intensity during scans. On the other hand, chemical saturation occurs below the detector threshold and is attributed to the fact that some probes will exhaust their binding capacities at relatively low concentrations, simply because their binding affinities are high. Binding affinities are in fact very sensitive to the sequence composition, resulting in measured brightnesses that usually vary by several orders of magnitude within a given probeset (Naef *et al.*, 2002). In addition, the systematic preference of $\approx 30\%$ of targets to the *MM* probes (measured *MM* intensities larger than *PM*s) has caused widespread confusion. Reasons for this phenomenon seem to lie beyond the anticipated decrease in binding energies resulting from the single substitution (Bonnet *et al.*, 1999; Vesnaver & Breslauer, 1991).

After presenting a detailed performance study of extant analysis methods, we present a method that achieves higher sensitivity at the high intensity end. The method is based on the notion that the probesets (*PM* and *MM*) should be considered as a set with a broad range of affinities, rather than the traditional interpretation of the *PM*s being the signals and the *MM*s being non-specific controls. Indeed, it has become clear that the *MM* probes also track the signal, usually with lower (although often with higher) affinities than the *PM*s. In that sense, the *MM*s should be viewed as a set of on average lower affinity probes. Having this in mind, it is then reasonable to expect that some *MM* probes will track the signal better at higher intensities because they will not saturate as

rapidly as the *PM*s (cf. fig 3).

Methods

The existing methods for the analysis of the raw data fall into two main classes. The first methods are similar to Affymetrix’s Microarray Suite software, providing absolute intensities on a chip by chip basis, or differential expression ratios from two experiments (Affymetrix, 2001; Naef *et al.*, 2001; Naef *et al.*, 2002). The second class are called “model-based” approaches (Li & Wong, 2001), and attempt to fit the probe affinities from a large number of experiments. It is natural to expect that the second class should lead to more accurate results as it incorporates more data into the analysis; however, the first methods are still necessary as not every laboratory can afford to run the ideal number of 16-20 required chips at once. Our new method belongs to the second class and is based on ideas borrowed from the theory of locally linear embeddings (Roweis & Saul, 2000).

Notation

We construct the following matrix

$$A_i^j = \begin{cases} PM_i^j & 1 \leq j \leq N_p \\ MM_i^{(j-N_p)} & N_p < j \leq 2N_p \end{cases}$$

or in expanded notation

$$A_i^j = \begin{bmatrix} PM_1^1 & \cdots & PM_1^{N_p} & MM_1^1 & \cdots & MM_1^{N_p} \\ \vdots & & \vdots & \vdots & & \vdots \\ PM_{N_e}^1 & \cdots & PM_{N_e}^{N_p} & MM_{N_e}^1 & \cdots & MM_{N_e}^{N_p} \end{bmatrix}$$

which contains the raw, *background subtracted* and *normalized data*. N_p is the number of probe pairs and N_e is the number of experiments. We introduce a set of weights w_i such that

$$\sum_{i=1}^{N_e} w_i = 1$$

and define the column means (or center of mass)

$$m^j = \sum_{i=1}^{N_e} w_i \log(A_i^j)$$

Note, we are computing the mean of the logs of the components of A_i^j .

¹Figure 7 at http://www.affymetrix.com/products/algorithms_tech.html

Principal component analysis

Loosely speaking local embeddings are necessary because the non-linearities (resulting from chemical saturation) affect the one-dimensional manifold $\{PM^j(c), MM^j(c)\}$ (the concentration c is the one-dimensional 'curve' parameter) by giving it a non-zero local curvature. The results section contains ample evidence that these non-linearities are significant. Our method is a multidimensional generalization of the schematic depicted in Figure 2, which shows the typical situation of two probes in which one of the probes ($PM2$) saturates at concentrations lower than the other. If both probes were perfectly linear, the curve would be a straight line with slope 1. In the multidimensional case, the directions of largest variation (analogous to D1 or D2 in Figure 2) are computed from the principal components of the matrix

$$\sqrt{w_i} \left(\log(A_i^j) - m^j \right) = \sum_{k=1}^{N_p} U_{ik} D_k V_k^j$$

which can easily be done via singular value decomposition (SVD). In order to reconstruct the concentrations, one needs to consider the unspecified sign of the vector V_1^j (when returned by the SVD routine), which has to be chosen such that $\sum_{i,j} \log(A_i^j) V_1^j > 0$ (the total amount of signal cannot be negative). The signal s_i , corresponding to the logarithms of the concentrations, is then computed by projecting the original matrix onto the first principal component V_1^j , corrected by a factor v_{max} which accounts for the fact that the vector V_1^j is L_2 -normalized ($\sum_j (V_1^j)^2 = 1$) implicitly by the SVD procedure:

$$s_i = v_{max} \sum_{j=1}^{N_p} \log(A_i^j) V_1^j$$

where $v_{max} = \max_j |V_1^j|$. In addition, one automatically obtains a signal-to-noise measure for the entire probeset

$$\frac{S}{N} = \frac{D_1}{\sqrt{\sum_{j=2}^{N_p} D_j^2}},$$

where $\{D_k\}$ are the singular values. For the results shown in Figure 5, we used the following weights

$$w_i = \frac{1}{W} \begin{cases} 1, & \hat{s}_i > \Gamma, \\ 1/(1 + b(i - i_s)^2), & \hat{s}_i \leq \Gamma \end{cases}$$

where $W = \sum_i w_i$, \hat{s}_i is the signal obtained with uniform weights, $i_s = 20$ (out of 28 experiments), $b = 2$, and $\Gamma = \hat{S}_{i_s+1}$ with \hat{S}_i being the ascendantly

sorted $\{\hat{s}_i\}$. With this scheme, lower concentration points were suppressed according to their rank, using a slowly decaying Cauchy weight function. There are many other ways to choose the weights, we simply want to show a proof of principle here.

Note, the fitting procedure used in the Li-Wong (Li & Wong, 2001) method is identical to an SVD decomposition, however, with different input data than was used here. The three main differences between our method and the Li-Wong technique are: (i) in the analysis here, we used log transformed PM and MM intensities, rather than the bare $PM-MM$ values; (ii) we introduced optional weights, which can account for non-linearities of the probe response in the high concentration regime; (iii) we subtract the column mean before we compute the principal components, which is crucial for capturing the local directions of variation. Indeed, as can be seen in Figure 2, the principal component would be dominated by the mean itself without subtraction.

Results

Data sets

The yeast Latin square (LS) experiment is a calibration data set produced by Affymetrix, that uses a non-commercial yeast chip. 14 groups of 8 different genes, all with different probe sets, are spiked onto 14 chips at concentrations, in pM, corresponding to all cyclic permutations of the sequence (0, 0.25, 0.5, 1, 2, ..., 1024). Hence, each group is probed at 13 different finite concentrations, logarithmically spaced over a range of magnitudes from 1 to 4096 (in Figures 3 and 5, we refer to these concentrations as (1 = 0.25 pM, 2 = 0.5 pM ... 13 = 1024 pM), and each group is completely absent in one array. Besides the spiked-in target cRNA's, a human RNA background was added to mimic cross-hybridization effects that would occur in a real experiment. In addition, each experiment was hybridized twice leading to 2 groups of 14 arrays called R1 and R2. This data set was invaluable for initiating the analysis and in allowing us to validate the results.

Summary of two-array methods

The figures in the results section show the log-ratios as function of concentration in the form of boxplots. In these plots, the central rectangle indicates the median, 1st and 3rd quartiles ($Q1$ and $Q3$). The "whiskers" extend on either side up to the last point that is not considered an outlier. Outliers are explicitly drawn and are defined as laying outside the inter-

val $[Q1 - 1.5 * IQ, Q3 + 1.5 * IQ]$, where $IQ = Q3 - Q1$ is the interquartile distance. For each method, we show three plots, the top two measure the false negative rate for ratios of 2 and 4 fold respectively, and the last one shows the false positive rate. For the top two plots, all combinations (within R1 and R2 separately) of arrays leading to ratios of 2 and 4 were considered, and plotted as function of their baseline intensity (the lesser of the two concentrations). For the third, each gene was compared between the groups R1 and R2, at identical concentrations. Of the $8 * 14 = 112$ transcripts, 8 were left out of the analysis because they did not lead to a signal that was tracking the concentrations at all (presumably due to bad probes or transcript quality).

In Figures 3, we summarize the results obtained by the Microarray Analysis Suite 5.0 (MAS 5.0) software and the “2 chips” method discussed in (Naef *et al.*, 2002). The later method computes for each gene probed in two arrays a ratio score R such that

$$\log(R) = \sum_j^{robust} \log(R^j)$$

is a robust geometric mean (a least trimmed squares estimator) of the probe ratios R^j . Figure 3 shows the cases where

$$R^j = \frac{PM_1^j - MM_1^j}{PM_2^j - MM_2^j}$$

and

$$R^j = \frac{MM_1^j}{MM_2^j}$$

In both cases, only probes with numerator and denominator above background are retained. The first case ($PM - MM$) is in essence similar to the MAS 5.0 program, differences are in the choice of the robust estimator and in the treatment of negative differences. For our purpose here, we like to think of the new Affymetrix method as two-array, $PM - MM$ based method. In all the results presented below, the arrays were scaled according to the MAS 5.0 default settings.

The main features of Figure 3 are: there is an optimal range of baseline concentrations ($\approx 1 - 16$ pM) in which the ratio values from both $PM - MM$ methods (the two first columns) are fairly accurate, for both ratios of 2 and 4. For both lower and higher concentrations, there is a noticeable compression effect, which is most dramatic at the high end. At the highest baseline concentration (512 pM for the ratios of 2 and 256 pM for ratios of 4), changes of 2 are basically not detected and real changes of 4 are

compressed on average to values around 1.25. The analysis of the false positive rate (last row) shows that both methods yield very tight reproducibility: the log2 ratio distributions are well centered around 0 and the interquartile distances are roughly intensity independent and smaller than 0.2, meaning that 50% of the measurements fall in the ratio interval $[0.93, 1.07]$. To be fair, we should point out that as a ($PM - MM$) method, the MAS 5.0 algorithm is on average a bit cleaner, having slightly fewer outliers. However, we like to emphasize that the qualitative behavior in the two ($PM - MM$) methods is unchanged, especially as far as the high-intensity compression is concerned. Further, similar behavior is also found using the ($PM - MM$) Li-Wong method (data not shown). The above observations are consistent with what was reported recently in (Chudin *et al.*, 2001), confirming that these effects are independent of the chip series. In fact, we also have evidence from a similarly designed experiment with human chips that the compression effects are very similar and not better behaved (not shown).

The third column in Figure 3 illustrates our contention that the MM are in essence a set of lower affinity probes. We notice that using only the MM measurements in the two-array method changes the picture qualitatively. Whereas the low concentration regime is far worse than in the ($PM - MM$) methods, the behavior toward the high end has changed and the drop off occurs now at higher concentrations: approximately 256 pM for the ratios of 2 and 128 pM for ratios of 4. On the other hand, even in the optimal range, the magnitude of the medians are always a bit lower than the real ratios, and the false positive rate also suffers. To summarize, this result suggests that if one is interested in accuracy at high concentrations, then the MM -only methods offers the best two-array alternative. We have tried other variations: PM only, or the double size set consisting in the merged PM and MM s, both being worse at high concentrations than the MM only method.

Although ratio score may suffer severe compression, there remains the possibility that they would be attributed a significant increase or decrease call. Figure 4 displays the relation between the MAS 5.0 log-ratios and their associated p-values. MAS 5.0 change ‘p-values’ p_M are symmetric about 0.5 and designed such that the ratio score is called increased when $p_M < \gamma_1$ and decreased (D) when $p_M > 1 - \gamma_1$, with a default $\gamma_1 = 0.0025$. This definition is not well suited for plotting purposes, we therefore work with $p_{MAS} = p_M$ when $p_M < 0.5$, and $p_{MAS} = 1 - p_M$ otherwise. This way, both I and D genes have $p_{MAS} <$

γ_1 , the direction being given by the sign of the log-ratio. The results show that there remarkably few false positive calls: only 4 out of 624 for concentrations $c \leq 8$ pM, and 6 of 728 when $c \geq 16$ pM. Fold changes of 4 are also well detected despite the compression at high intensities: there are 21 false negatives (and 3 false positives having ratios with the wrong sign) out of 1248 for $c \leq 8$ pM, and 84 of 1040 false negatives for $c \geq 16$ pM. The situation deteriorates for fold changes of 2, with 124 false negatives (and 3 false positives) out of 1248 for $c \leq 8$ pM, and 425 of 1248 false negatives for $c \geq 16$ pM.

Multi-array methods

The data analyzed using our new method is shown in Figure 5. It is clear that both are capable of reducing the high intensity compression, as compared to existing methods. The second column explicitly shows what can be gained from the local embedding. It should be noted, however, that the false positive rate is significantly larger than with the MAS 5, which is not surprising as this technique is designed to maximize the signal detection. As compared to the “two chip” *MM* method, which was previously the least compressive in this regime, the medians are systematically more accurate.

Discussion

There are two orthogonal ways to utilize and think about microarray experiments. In the first case, one may wish to minimize the false positive rate, and we’ve shown that the new MAS 5.0 algorithm is does remarkably well in that respect. On the other hand, using microarrays as a gene discovery tool is perhaps their most attractive feature. In that sense, it is desirable to have methods aimed at maximizing sensitivity, at the expense of a larger false positive rate. It is expected in this case that microarray studies would be independently verified to control for the increase in false positives. Additionally, we often hear from scientists that wildly different conditions, like severe pharmaceutical treatments or gene knockouts, appear to have no detectable transcriptional effects. While there is indeed the possibility that transcription regulatory networks can compensate for such changes, or that some effects would be mostly post-transcriptional, real transcriptional changes may also be masked by compressive effects like those discussed above.

As we have shown, finer methods offer the potential to recover some of the lost signal, however, strong enough non-linearities and compression will always

win in the end. Therefore, the real bottleneck currently resides in the technology itself, and also in our limited understanding of the physical chemistry governing oligonucleotide hybridizations, as discussed in detail in (Naef *et al.*, 2002). Advances in this area, as can be expected after the release of the probe sequences by Affymetrix will greatly aide both the design and data analysis steps. As far as design issues are concerned, probe selection is likely to be a crucial aspect. Nevertheless, meeting the desired linearity over, say 4 decades in concentration, together with the constraint on high specificity of short length probes will certainly be a difficult challenge.

Conclusions

We have summarized in detail the performance of existing methods for analyzing Affymetrix GeneChip data, using the yeast calibration dataset we were fortunate to obtain from Affymetrix. The results show unambiguously the compressive tendency of conventional methods in the high-intensity range, namely that fold changes as large as 4 in expression levels can be reduced to fold changes barely larger than 1 (Figure 3). Additionally, we have proposed a new method that enables one to extract more signal at high concentrations. One caveat at this point is that while achieving better accuracy at high intensities, our method presented here performs worse than traditional methods at low-intensities. In that regime, it seems that the best results are obtained from the usual *PM* – *MM* scheme. This indicates that GeneChip data is sufficiently complex enough that for optimal performance, radically different approaches may have to be used in the low and high intensity ranges. It is plausible, however, that there may be a technique that optimally interpolates between the two regimes.

Acknowledgments

The authors are very thankful to Affymetrix for having provided the precious calibration data. F. N. is a Bristol-Meyers Squibb Fellow and acknowledges support from the Swiss National Science Foundation. This work was also supported by NIH/NINDS Grant NS39662 (N. D. S) and the Meyer Foundation (M. M.)

References

- Affymetrix (2001) *Affymetrix Microarray Suite 5.0 User Guide*. Affymetrix, Inc., Santa Clara, CA.
- Bonnet, G., Tyagi, S., Libchaber, A. & Kramer, F. R. (1999) Thermodynamic basis of the enhanced specificity of structured DNA probes. *Proc. Natl. Acad. Sci. U. S. A.*, **96** (11), 6171–6176.
- Chee, M., Yang, R., Hubbell, E., Berno, A., Huang, X. C., Stern, D., Winkler, J., Lockhart, D. J., Morris, M. S. & Fodor, S. P. (1996) Accessing genetic information with high-density DNA arrays. *Science*, **274** (5287), 610–614.
- Chudin, E., Walker, R., Kosaka, A., Wu, S. X., Rabert, D., Chang, T. K. & Kreder, D. E. (2001) Assessment of the relationship between signal intensities and transcript concentration for affymetrix genechip(r) arrays. *Genome Biol.*, **3** (1), Research0005.
- Li, C. & Wong, W. H. (2001) Model-based analysis of oligonucleotide arrays: expression index computation and outlier detection. *Proc. Natl. Acad. Sci. U. S. A.*, **98** (1), 31–36.
- Lipshutz, R. J., Fodor, S. P., Gingeras, T. R. & Lockhart, D. J. (1999) High density synthetic oligonucleotide arrays. *Nat. Genet.*, **21** (1 Suppl), 20–24.
- Naef, F., Hacker, C. R., Patil, N. & Magnasco, M. (2002) Empirical characterization of the expression ratio noise structure in high-density oligonucleotide arrays. *Genome Biol.*, **3** (1), in press.
- Naef, F., Lim, D. A., Patil, N. & Magnasco, M. (2001) From features to expression: high-density oligonucleotide array analysis revisited. In *Proceedings of the DIMACS Workshop on Analysis of Gene Expression Data* The American Mathematical Society.
- Naef, F., Lim, D. A., Patil, N. & Magnasco, M. (2002) DNA hybridization to mismatched templates: a chip study. *Phys. Rev. E*, **to appear in the April 1rst edition**.
- Roweis, S. T. & Saul, L. K. (2000) Nonlinear dimensionality reduction by locally linear embedding. *Science*, **290** (5500), 2323–2326.
- Vesnaver, G. & Breslauer, K. J. (1991) The contribution of DNA single-stranded order to the thermodynamics of duplex formation. *Proc. Natl. Acad. Sci. U. S. A.*, **88** (9), 3569–3573.

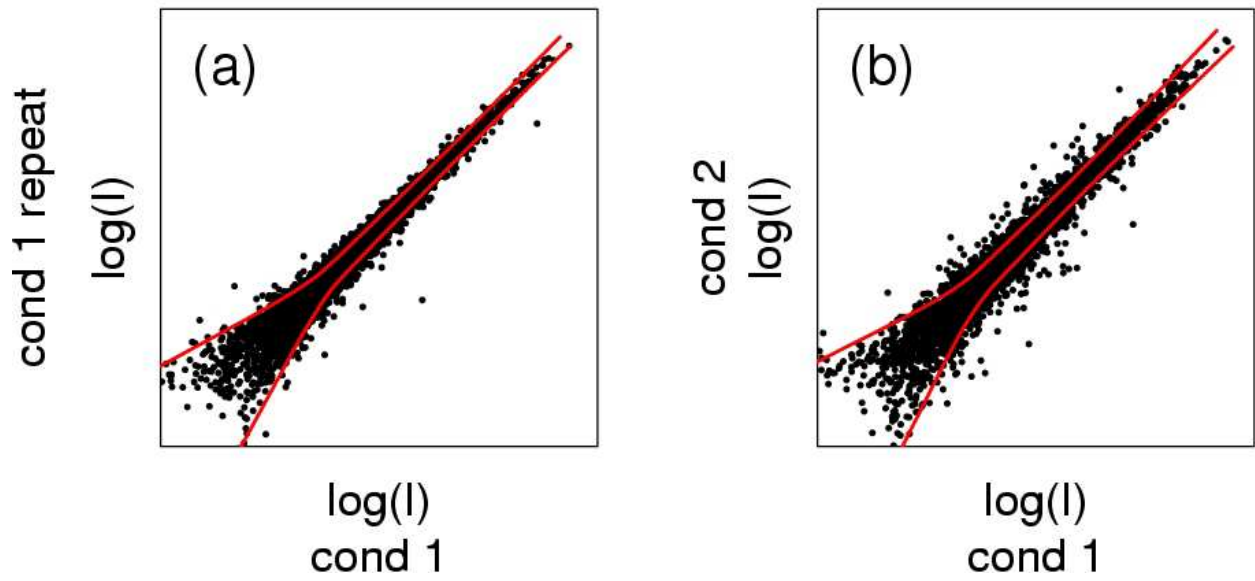


Figure 1: Typical scatterplots from GeneChip data. a) Log transformed intensities for repeated hybridization conditions (duplicates). b) different conditions. The red lines show the lines of local $SD=2$.

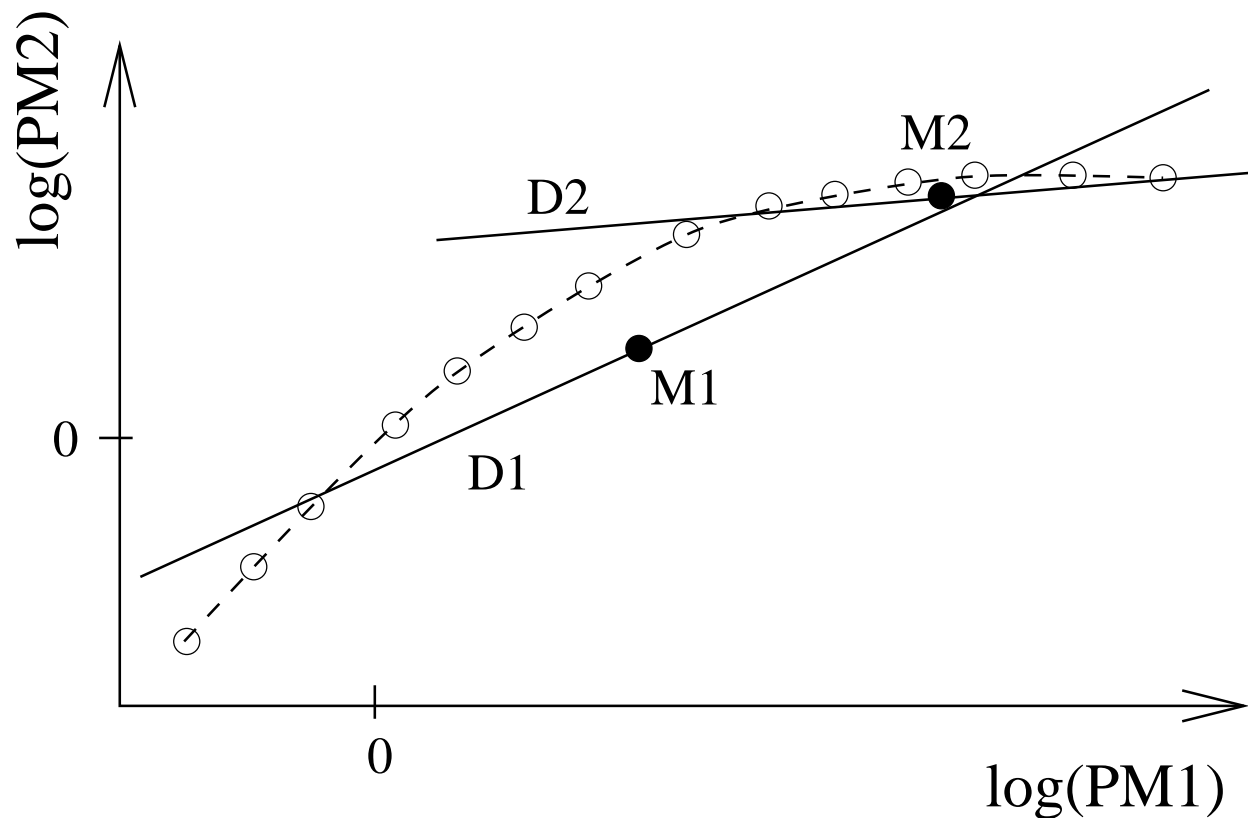


Figure 2: Typical compressive situation: a 2 dimensional cartoon. The open dots represent fictitious measurement of two probes (PM1, PM2) at increasing concentrations (from left to right). Probe PM2 saturates earlier than PM1. $M1 = (m^1, m^2)$ represents the mean with uniform weights $\{w_i\}$ and $M2$ a mean obtained with weights that are larger for high concentrations. $D1$ and $D2$ show the corresponding principal components (direction of largest variance). It is clear that projecting the points onto $D1$ has the effect of a compression due to the curvature. On the other hand, this compression is largely reduced at high-intensities by projecting onto $D2$.

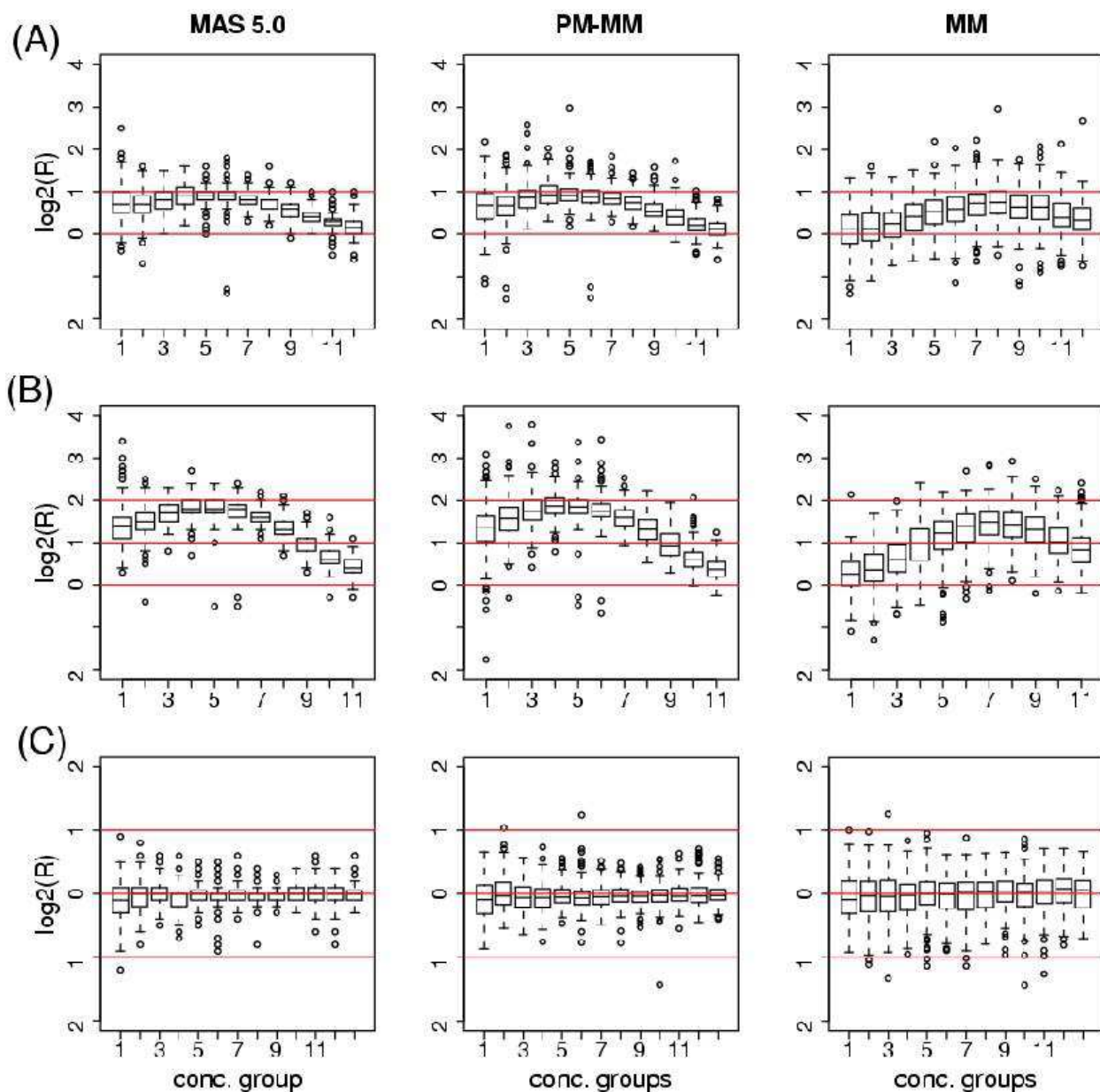


Figure 3: Comparison of 'two array' methods: MAS 5.0 (first column), *PM* – *MM* (second) and *MM*only (third) of (Naef *et al.*, 2002). Boxplots show the log base 2 ratio distributions for each baseline concentration group (cf. text). Row A: Fold change of 2, B: Fold change 4, C: Negative controls (false positives). The central rectangle indicates the median, 1st and 3rd quartiles ($Q1$ and $Q3$). The “whiskers” extend on either side up to the last point which is not considered to be an outlier. Outliers are explicitly drawn and are defined as laying outside the interval $[Q1 - 1.5 * IQ, Q3 + 1.5 * IQ]$, where $IQ = Q3 - Q1$ is the interquartile distance. Notice the two first rows are qualitatively similar, with the MAS 5.0 being marginally cleaner. Both methods show a strong high concentration compression, but have excellent reproducibility (cf. text). The third column illustrates that MM probes contain valuable signal, often leading to more accurate ratios at high concentrations.

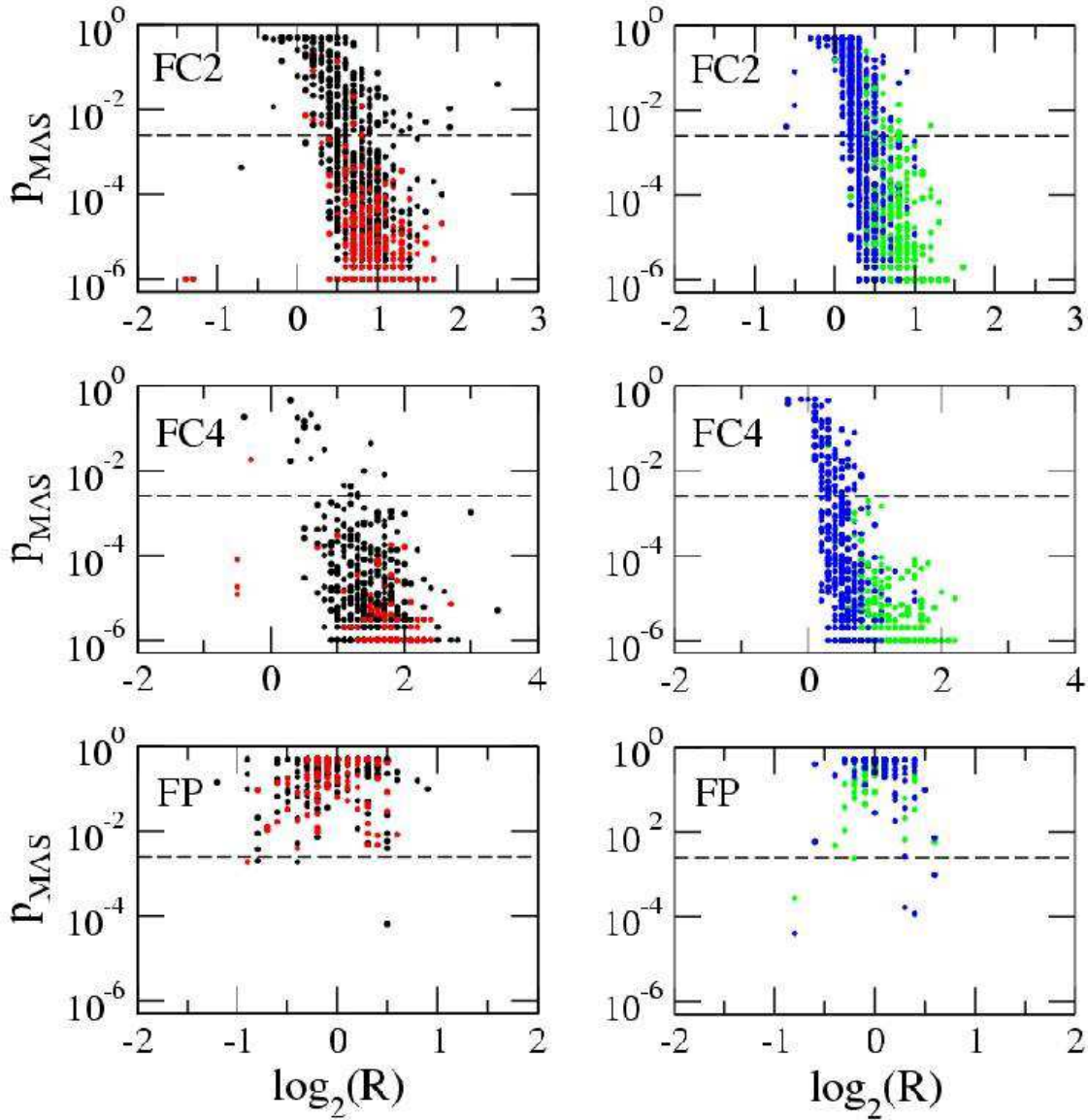


Figure 4: P-values vs. log-ratios in for MAS 5.0. The plotted p_{MAS} is the transformed MAS 5.0 p-value (cf. text). The dotted line indicates the default $\gamma_1 = 0.0025$, below which MAS 5.0 scores are considered increased (I) or decreased (D) (for the transformed p-value). Colors are used to group baseline intensities of 0.25–1 pM (black), 2–8 pM (red), 16–64 pM (green), 128–1024 (blue).

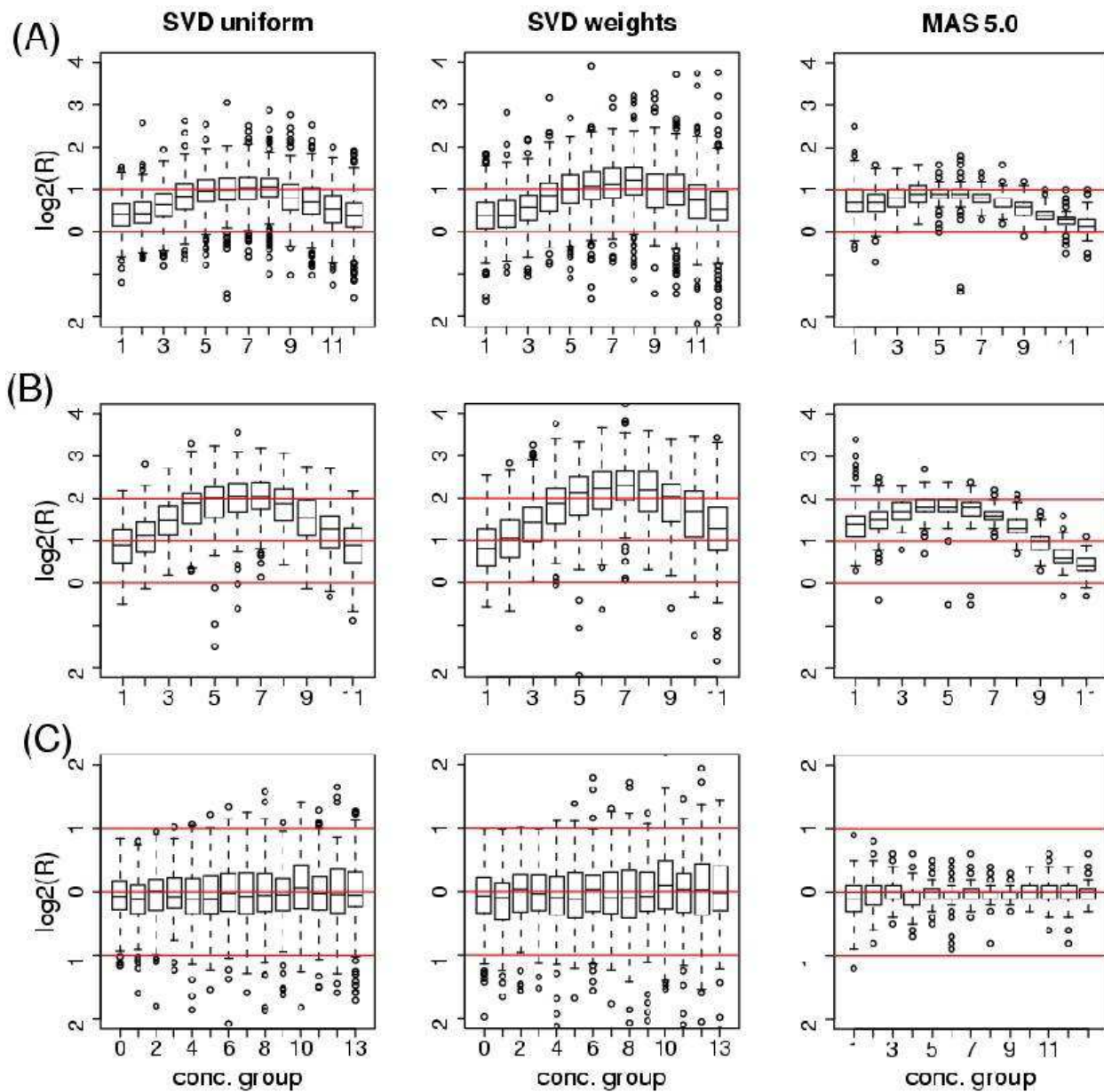


Figure 5: Rows are as in Figure 3, columns show the new method with uniform (first column), Cauchy weights introduced in the text (second), and the reference MAS5.0 (third).